Inhibition of Hematopoietic Protein Tyrosine Phosphatase Augments and Prolongs ERK1/2 and p38 Activation

Eduard Sergienko,[‡,#] Jian Xu,[§,#] Wallace H. Liu,[†] Russell Dahl,[‡] David A. Critton,[⊥] Ying Su,[‡] Brock T. Brown,[‡] Xochella Chan,[‡] Li Yang,[‡] Ekaterina V. Bobkova,[‡] Stefan Vasile,[‡] Hongbin Yuan,[‡] Justin Rascon,[‡] Sharon Colayco,[‡] Shyama Sidique,[‡] Nicholas D. P. Cosford,[‡] Thomas D. Y. Chung,[‡] Tomas Mustelin,[†] Rebecca Page,[⊥] Paul J. Lombroso,[§,‖] and Lutz Tautz[†,*]

[†]Infectious and Inflammatory Disease Center and [‡]Conrad Prebys Center for Chemical Genomics, Sanford-Burnham Medical Research Institute, La Jolla, California 92037, United States

[§]Child Study Center and [‖]Departments of Psychiatry and Neurobiology, Yale University School of Medicine, New Haven, Connecticut 06520, United States

[⊥]Department of Molecular Biology, Cell Biology, and Biochemistry, Brown University, Providence, Rhode Island 02912, United States

ⓢ *Supporting Information*

ABSTRACT: The hematopoietic protein tyrosine phosphatase (HePTP) is implicated in the development of blood cancers through its ability to negatively regulate the mitogen-activated protein kinases (MAPKs) ERK1/2 and p38. Small-molecule modulators of HePTP activity may become valuable in treating hematopoietic malignancies such as T cell acute lymphoblastic leukemia (T-ALL) and acute myelogenous leukemia (AML).

Moreover, such compounds will further elucidate the regulation of MAPKs in hematopoietic cells. Although transient activation of MAPKs is crucial for growth and proliferation, prolonged activation of these important signaling molecules induces differentiation, cell cycle arrest, cell senescence, and apoptosis. Specific HePTP inhibitors may promote the latter and thereby may halt the growth of cancer cells. Here, we report the development of a small molecule that augments ERK1/2 and p38 activation in human T cells, specifically by inhibiting HePTP. Structure–activity relationship analysis, *in silico* docking studies, and mutagenesis experiments reveal how the inhibitor achieves selectivity for HePTP over related phosphatases by interacting with unique amino acid residues in the periphery of the highly conserved catalytic pocket. Importantly, we utilize this compound to show that pharmacological inhibition of HePTP not only augments but also prolongs activation of ERK1/2 and, especially, p38. Moreover, we present similar effects in leukocytes from mice intraperitoneally injected with the inhibitor at doses as low as 3 mg/kg. Our results warrant future studies with this probe compound that may establish HePTP as a new drug target for acute leukemic conditions.
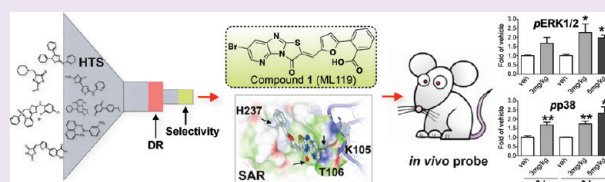
Tyrosine phosphorylation[1] is a key mechanism for signal transduction and the regulation of a broad set of physiological processes characteristic of multicellular organisms. The importance of tyrosine phosphorylation in normal cell physiology is well illustrated by the many inherited or acquired human diseases that stem from abnormalities in protein tyrosine kinases (PTKs) and protein tyrosine phosphatases (PTPs).[2−5] Hematopoietic cells have particularly high levels of tyrosine phosphorylation and express more genes for PTKs and PTPs than any other cell type, with the possible exception of neurons.[3] Acute changes in tyrosine phosphorylation mediate antigen receptor-induced lymphocyte activation, leukocyte adhesion and migration, cytokine-induced differentiation, and responses to many other stimuli.

The MAPKs extracellular-signal regulated kinases 1 and 2 (ERK1/2), c-Jun N-terminal kinases 1, 2, and 3 (JNK1/2/3), and the α-, β-, γ-, and δ-isoforms of p38 act as integration points in the signaling cascades of hematopoietic cells.[6] These kinases are ultimately activated *via* dual phosphorylation of a threonine and a tyrosine residue in their activation loop.[7] The human genome encodes 11 typical MAPK phosphatases (MKPs), which inactivate MAPKs by dephosphorylating the phosphotyrosine (*p*Tyr) and phosphothreonine (*p*Thr) residues in their T-X-Y motif.[8] In addition, several atypical dual-specific PTPs, including VHR[9] and VHX,[10] as well as the Ser/Thr phosphatase PP2A,[11,12] dephosphorylate MAPKs. The reason for this abundance of phosphatases relates to the numerous critical roles of MAPKs in the cell and the profound effects of the duration of MAPK activation on cell physiology. To achieve some degree of specificity, MAPK-specific phosphatases (1) reside in different subcellular locations, (2) are subject to different modes of post-translational regulation,

(3) use different mechanisms for association, and (4) are expressed in response to different stimuli and in lineage-specific manners. Thus, while MAPK activation is the result of a conserved kinase cascade, several phosphatases serve as negative regulators in a temporal, spatial, and cell-type-specific manner.[6,13]

HePTP (*PTPN7*)[14,15] is the only *p*Tyr-specific PTP known to dephosphorylate MAPKs in hematopoietic cells. HePTP is a 38-kDa enzyme, consisting of the C-terminal catalytic PTP domain and a short (~45 residues) N-terminal extension, which contains the kinase interaction motif (KIM, residues 15−31). *Via* its KIM, HePTP tightly associates with its physiological substrates including the MAPKs ERK1/2 and p38.[16−18] In resting T cells, HePTP dephosphorylates the positive regulatory *p*Tyr residue in the activation loop of these kinases[16,17] and prevents their translocation to the nucleus.[17,19] T cell antigen receptor (TCR) ligation leads to the activation of MAPKs, as well as to the phosphorylation of HePTP at residue Ser23 by cAMP-dependent kinase (also known as protein kinase A, PKA).[20] This causes a significant fraction of the HePTP/MAPK molecules to dissociate,[17] enabling activated, unbound ERK/p38 to translocate to the nucleus and initiate transcription events that are required for T cell activation. Some 30−60 min later, several MKPs accumulate in the nucleus and dephosphorylate ERK/p38.[6] The inactivated MAPKs subsequently shuttle back to the cytosol and reassociate with HePTP. This dual phosphatase regulation of ERK/p38 is referred to as the "sequential phosphatase model"[6] and is an example of how different PTPs are used in a spatially and temporally ordered manner to control the extent, location, and duration of MAPK activation (Figure 1).
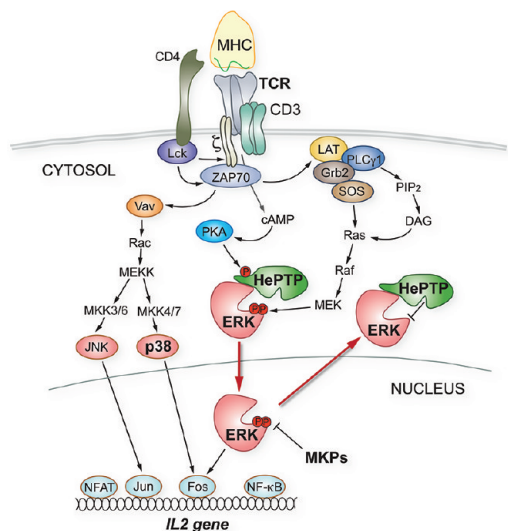

Figure 1. TCR-induced MAPK signaling. The "sequential phosphatase model" is illustrated for the MAPK ERK1/2. This model also applies to the MAPK p38, which undergoes similar interactions with HePTP.

HePTP is expressed in bone marrow, thymus, spleen, lymph nodes, and in all myeloid and lymphoid lineages and cell lines.[14,15,21] The HePTP gene is located on chromosome 1q32[22] and is often duplicated in bone marrow cells from patients with myelodysplastic syndrome (MDS),[23,24] which is characterized by disturbed hematopoiesis and an increased risk of acute leukemia. Amplification and overexpression of HePTP is also reported in cases of acute myeloid leukemia (AML).[22]

Searching the Oncomine database, we found that HePTP mRNA levels are significantly upregulated in AML and also in T cell acute lymphoblastic leukemia (T-ALL) (Supplementary Figure S1). Because HePTP expression is restricted to hematopoietic lineages, it is a potential target for the development of novel therapeutics directed toward diseases of the blood and the immune system.

Specific small molecule modulators of HePTP activity have only recently been described.[25,26] Such compounds are thought to augment ERK1/2 and p38 activation and may cause a sustained hyperactivation of these MAPKs. In light of recent reports showing that prolonged activation of the Raf-Ras-ERK pathway can result in cell cycle arrest and cell senescence[13] and the fact that p38 can negatively regulate cell cycle progression and activate apoptotic pathways,[27] HePTP inhibitors are of interest in the search for new leukemia therapeutics. In addition, such compounds will be useful for further elucidating the mechanisms of MAPK regulation and lymphocyte activation. Here, we report the development of a specific inhibitor of HePTP activity in human T cells. We demonstrate the structural basis for HePTP inhibition and show that interactions of the compound with unique amino acid residues in the HePTP substrate-binding loop and WPD-loop are critical for inhibitor binding and selectivity. Moreover, we show that the compound is active *in vivo*, augmenting activation of the MAPKs ERK1/2 and p38 in white blood cells from mice injected with a low dose of the inhibitor. Importantly, we demonstrate that pharmacological inhibition of HePTP not only augments but also prolongs the activation of the MAPKs ERK1/2 and p38.

■ RESULTS AND DISCUSSION

Potent and selective small molecules that perturb a physiological target in a dose-dependent manner can be used to probe the role of the target in biology. Compared to mutant organisms that are often able to compensate for the loss of a gene, chemical probes can rapidly penetrate into cells, bind to their target proteins, and create loss-of-function (or gain-of-function) phenotypes. Such compounds can be administrated at any time during development and at any desired location of the cell or organism. Thus, chemical probes provide temporal and spatial control over their protein targets, and techniques such as activity-based protein profiling have emerged as powerful strategies.[28] However, the successful generation and application of such molecules remains challenging.[29] This is particularly true when targeting members of enzyme classes with highly conserved catalytic cores, such as PTPs.[30−32] HePTP is an important negative regulator of the MAPKs ERK1/2 and p38 in hematopoietic cells. Protein and mRNA expression levels are upregulated in cells from patients with preleukemic conditions or acute leukemia. HePTP chemical probes can be utilized to study the effects of HePTP inhibition on ERK1/2 and p38 activation in hematopoietic cells. If such compounds are able to augment and sustain MAPK activation levels, they may lead to new strategies in leukemia therapy.

High-Throughput Screening (HTS) for HePTP Inhibitors. HePTP was screened within the Molecular Library Screening Center Network (MLSCN). The primary HTS and dose−response confirmation assays utilized the generic phosphatase substrate *p*-nitrophenyl phosphate (*p*NPP).[30] In our reaction, product phosphate was quantified using the colorimetric malachite green-based Biomol Green reagent. The assay conditions were optimized for HTS in 384-well format

(Supplementary Figure S2). Screening parameters were determined and indicated a robust and reliable HTS assay; the average Z was 0.8, the signal to background ratio was 6.4, the signal-to-noise ratio was 300, and the signal window was 12.3. A total of 112,438 compounds were screened at a concentration of 20 μM, and 54 hit compounds were found to dose-dependently inhibit HePTP activity with IC$_{50}$ values lower than 10 μM. Chemical similarity clustering by a Tanimoto distance[33] of 0.5 resulted in 28 different clusters and singletons, indicating a quite diverse chemical space covered by these molecules (Figure 2). Detailed screening results, including a
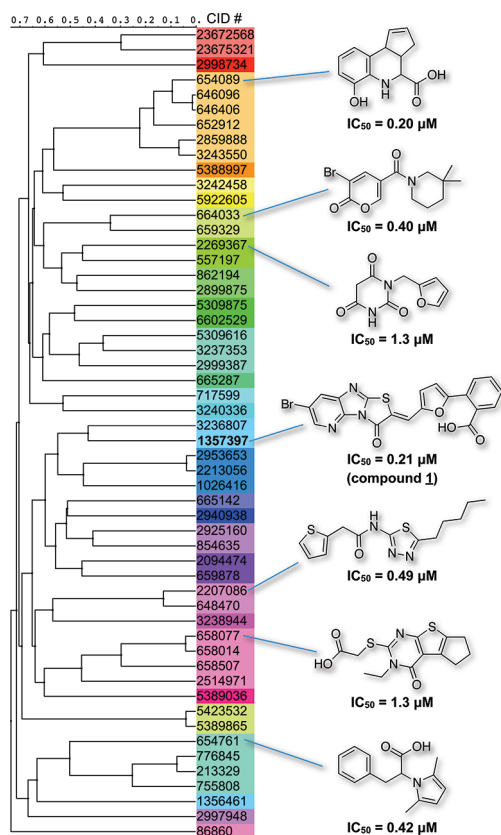

Figure 2. Chemical similarity clustering of the 54 confirmed HePTP screening hits with IC$_{50}$ values <10 μM. Compounds are listed by their PubChem Chemical ID number (CID), clustered by a Tanimoto distance of 0.5, and linked using the UPGMA method. Representative compounds and their respective IC$_{50}$ values for HePTP are shown to demonstrate the chemical diversity of the HTS hits. A complete list of the chemical structures can be found on the PubChem Web site (http://pubchem.ncbi.nlm.nih.gov/), under AID 521.

complete list of the screening hits and the confirmatory assay data, were deposited at the PubChem Web site (http://pubchem.ncbi.nlm.nih.gov/) under BioAssay ID (AID) 521.

Since the catalytic mechanism of PTPs involves a nucleophilic attack by the thiolate ion of a catalytic cysteine residue, PTPs are prone to inhibition by oxidizing agents or Michael-acceptor compounds. In order to test for this unwanted inhibition, a secondary assay was adapted using 3-O-methylfluorescein phosphate (OMFP), which is hydrolyzed into the fluorescent 3-O-methylfluorescein and phosphate (Supplementary Figure S3). With this continuous assay in place, progress curves of the reaction could be easily acquired and utilized for removing time-dependent inhibitors. Impor-

tantly, at this stage compounds were also evaluated for their relative selectivity to inhibit HePTP over the phosphatase MKP-3, which shares with HePTP the physiological targets ERK1/2. In these assays, the majority of compounds demonstrated similar activity against both HePTP and MKP-3 and thus were discarded from further consideration owing to lack of selectivity. However, one compound (compound 1, PubChem CID1357397, NIH MLP probe number ML119) selectively inhibited HePTP over MKP-3 by 25-fold (Table 1). Compound 1 inhibited HePTP catalytic activity with an IC$_{50}$ value of 0.21 μM. HePTP activity progress curves were linear over 98 min at different concentrations of compound 1, indicating no time-dependent inhibition of the enzyme (Figure 3a). Michaelis−Menten kinetic studies at various inhibitor and substrate concentrations revealed a mixed inhibition pattern for compound 1 with predominantly competitive participation and a competitive inhibition constant of $K_i = 0.211 \pm 0.250$ μM (Figure 3b). Taken together, HTS yielded a potent compound with a 25-fold greater inhibition of HePTP compared to MKP-3 and with a primarily competitive inhibition pattern, suggesting a binding mode that involves the active site/catalytic pocket.

Structure−Activity Relationship (SAR) Analysis of Compound 1 Using Chemical Analogues. In order to elucidate the molecular basis for inhibition of HePTP, the SAR for compound 1 was developed around the thiazolo[2',3':2,3]-imidazo[4,5-b]pyridin-3(2H)-one scaffold scaffold (Table 1). Dose−response phosphatase assays, using OMFP as a substrate, were performed to determine IC$_{50}$ values for each analogue. Since the majority of reported PTP inhibitors contain a structural element that binds to the phosphate-binding loop (P-loop) at the base of the catalytic pocket by mimicking pTyr,[30] we expected the negatively charged benzoic acid group of compound 1 to be essential for inhibition. Indeed, HePTP IC$_{50}$ values of compound 1 analogues clearly supported such a binding mode, in which the benzoic acid functions as a pTyr mimetic. Replacing the carboxylic acid with a nitro group (compound 3) or chlorine substituents (compound 4) reduced inhibitory activity by more than 20-fold. Replacing the bromine substituent at the other end of the molecule with methyl groups (compound 2) resulted in an 8.5-fold higher IC$_{50}$ value (Table 1). Notably, analogues of compound 1 that were significantly smaller because they lacked the furanyl ring and that did not carry a carboxylic acid group showed moderate or no activity against HePTP (compounds 5 and 6). Also, benzoic acid alone did not inhibit HePTP, even at high micromolar concentrations. Thus, SAR analysis suggests that compound 1 uses an o-benzoic acid group to bind into the catalytic pocket of HePTP, while additional interactions between inhibitor and protein surface are necessary for potency.

***In Silico* Docking Confirms SAR Analysis.** To investigate the interactions of compound 1 with the HePTP active site on an atomic level, flexible ligand docking with the HePTP crystal structure (PDB code 3D44, ref 34) was performed using the ICM docking algorithm.[41] The data from the docking studies support a binding mode in which the benzoic acid group in compound 1 functions as a pTyr mimetic. The benzoic acid was found to undergo multiple hydrogen bond interactions with residues of the PTP signature motif (H/V)CxxGxxR(S/T) of the P-loop (Figure 4). Additional hydrogen bond interactions near the catalytic center involved the side chain of the conserved Gln314 of the Q-loop as well as the imidazole group of His237 of the WPD-loop. As expected, compound 1 was

Table 1. SAR and Selectivity Analysis for Compound 1 and Analogues (IC$_{50}$ Values in μM)

Cmpd #	PubChem CID	Structure	HePTP	MKP-3	VHR	STEP	PTP-SL	PTP1B	LYP	TCPTP	SHP1	SHP2	CD45	LAR
1*	1357397*		0.21	5.2	1.9	6.3	1.1	1.7	1.9	1	2.5	1.1	3.1	73
2	5341943		1.8	17	5.8	~100	20	28	30	n/d	n/d	n/d	n/d	n/d
3	5341934		4.9	57	12	>100	41	~100	~100	n/d	n/d	n/d	n/d	n/d
4	2300608		5.7	>100	8.8	>100	~100	>100	>100	n/d	n/d	n/d	n/d	n/d
5	2258411		35	>100	>100	>100	>100	>100	>100	n/d	n/d	n/d	n/d	n/d
6	n/a		>100	>100	>100	>100	>100	>100	>100	n/d	n/d	n/d	n/d	n/d

* Compound 1 was submitted as a probe to the Molecular Libraries Probe Production Centers (MLPCN) and has the Probe ML# ML119.

found to interact with residues peripheral to the catalytic pocket. These interactions included hydrogen bonds between oxygen and nitrogen atoms of the heterocycle and the side chain of T106 of the substrate-binding loop (SB-loop), as well as favorable polar contacts between the bromine atom of the inhibitor and the ε-amino group of Lys105 in the HePTP SB-loop. We found similar interactions with residues of the SB-loop crucial for the selectivity of previously reported HePTP inhibitors.[25] In silico docking with the crystal structure of MKP-3 revealed a lack of such additional interactions with residues in the periphery of the catalytic pocket, perhaps explaining the substantially lower inhibitory activity of compound 1 against MKP-3. Neither Lys105 nor Thr106 of the HePTP SB-loop is conserved in MKP-3, which is missing a corresponding loop. Together, the in silico docking is in agreement with the SAR analysis and suggests that interactions of compound 1 with Lys105 and Thr106 contribute to the 25-fold selective inhibition of HePTP over MKP-3.

Mutagenesis Studies Confirm the Proposed Binding Mode for Compound 1. To further explore the binding mode of compound 1, we first used site-directed mutagenesis to mutate Lys105 and Thr106 to alanines and tested compound 1 against the recombinant HePTP double mutant (HePTP-DM). Using OMFP as a relatively small artificial substrate, we showed that kinetic parameters such as K_m and V_{max} were similar between wild-type (wt) and mutant protein, which allowed us to directly compare IC$_{50}$ values of the inhibitor. Compound 1 was 31-fold less active against HePTP-DM (IC$_{50}$ = 6.6 μM, Figure 3c) as compared to wt HePTP. These results suggest that Lys105 and Thr106 are important for the binding of compound 1 to HePTP.

Since His237 had not been implicated for compound binding in previous studies with HePTP inhibitors,[25] we also used site-directed mutagenesis to mutate His237 to alanine. We generated the recombinant HePTP H237A mutant and subjected the protein to inhibition studies with compound 1. Again, as predicted by the in silico docking studies, we found His237 of the HePTP WPD-loop important for inhibitor

binding. Compound 1 was more than 13-fold less active against the H237A mutant (IC$_{50}$ = 2.8 μM, Figure 3c) compared to wt HePTP. Thus, the mutagenesis studies confirm the proposed binding mode for compound 1.

Selectivity Profiling of Compound 1 and Analogues against Related PTPs. To evaluate the selectivity of compound 1 and analogues more broadly, a large panel of additional related PTPs was employed, including VHR, STEP, PTP-SL, PTP1B, LYP, CD45, SHP1, SHP2, TCPTP, and LAR. VHR, together with MKP-3 and HePTP, shares the common physiological targets ERK1/2. STEP and PTP-SL are the closest relatives of HePTP and together represent the subfamily of KIM-containing PTPs. PTP1B is the prototypical PTP and a critical regulator of essential pathways such as insulin and leptin signaling. LYP, CD45, SHP1, SHP2, TCPTP, and LAR are critical signaling molecules in lymphocytes, where HePTP is enriched. Using the dose−response OMFP phosphatase assay, we showed that compound 1 was a weaker inhibitor of all additionally tested PTPs compared to HePTP (Table 1). Compound 1 selectively inhibited HePTP over PTP-SL, SHP2, and TCPTP (5-fold), PTP1B (8-fold), VHR (9-fold), LYP (9-fold), SHP1 (12-fold), CD45 (15-fold), STEP (30-fold), and LAR (348-fold). In particular, the high preference of 1 for HePTP over STEP, one of its two most similar relatives (53% sequence identity within the PTP domain), was surprising. HePTP, PTP-SL, and STEP have almost identical active sites, based on sequence similarity. They differ only in the two residues that immediately follow the aspartic acid of their WPD-loops. In HePTP these residues are His237 and Gln238, in PTP-SL His555 and Lys556, and in STEP Gln462 and Lys463. In addition, the crystal structure of STEP (PDB code 2BV5, ref 26) reveals a different WPD-loop conformation, with the corresponding Gln462 pointing in the opposite direction, compared to His237 or His555 in HePTP and PTP-SL, respectively. Since our in silico docking and mutagenesis studies suggested that His237 contributes to inhibitor binding, selectivity of compound 1 over STEP is likely the result of
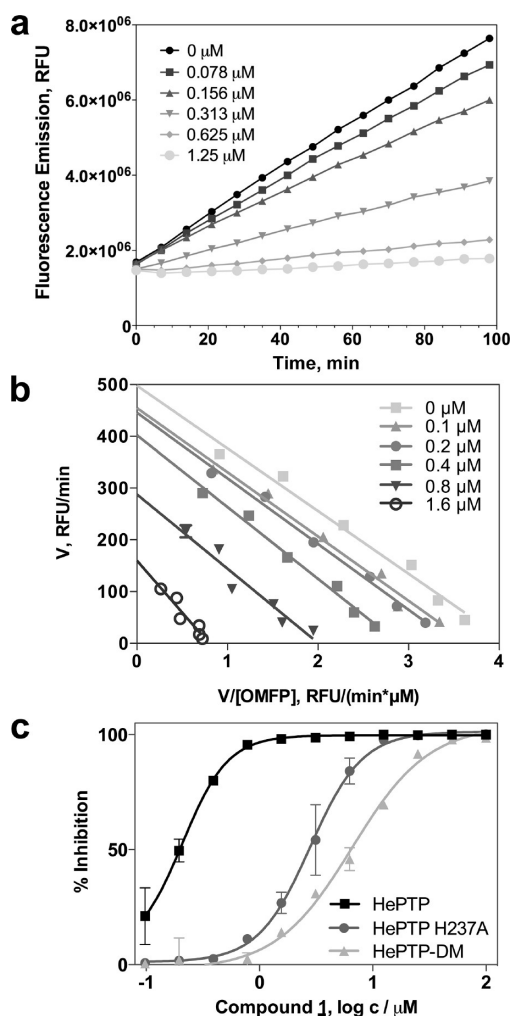
Figure 3. Mechanism of action (MOA) and inhibition studies of compound **1** with HePTP and HePTP mutants. (a) Progress curves of HePTP activity in the presence of different doses of compound **1**. No time-dependent inhibition was observed as demonstrated by the linear progress curves of the HePTP phosphatase reaction. (b) Eadie−Hofstee plot of the Michaelis−Menten kinetic studies with compound **1**. (c) Dose−response curves for compound **1** with either wt HePTP, HePTP-DM, or HePTP H237A.
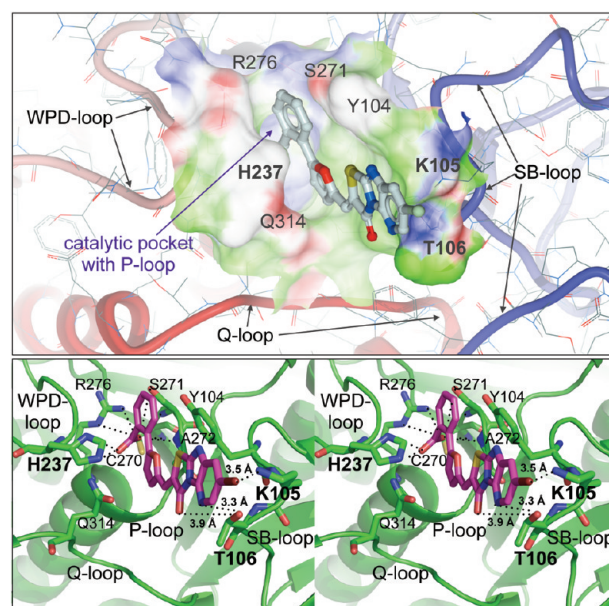

Figure 4. *In silico* docking of compound **1** into the HePTP active site. Upper panel: Ribbon and surface representation of the HePTP active site (crystal structure, PDB code 3D44) with docked inhibitor (stick representation). Surface color code: white, neutral; green, hydrophobic; red, hydrogen bond acceptor potential; blue, hydrogen bond donor potential. Lower panel: Stereo ribbon diagram of the docking pose used in the upper panel. Residues that interact with compound **1** (magenta) and the catalytic cysteine (C270 in HePTP) are shown in stick representation.

the missing histidine residue at the corresponding position in STEP, an otherwise highly similar phosphatase.

Interestingly, residues Lys105 and Thr106 in the HePTP SB-loop are not conserved among PTPs. In fact, Thr106 is unique to the three KIM-containing phosphatases HePTP, PTP-SL, and STEP. While a Thr106 corresponding residue is missing in the dual-specificity phosphatases MKP-3 and VHR, the *p*Tyr-specific PTPs typically have an aspartic acid at the equivalent position. The favorable hydrogen bonding interactions between the hydroxyl group of Thr106 and the heterocycle of compound **1** cannot be formed with an aspartic acid residue in that position. Thus, interactions of compound **1** with Thr106 likely confer the observed selectivity for HePTP over the classical *p*Tyr-specific PTPs. Taken together, compound **1** is the most selective HePTP inhibitor reported to date. Given at the appropriate dosage, off-target effects on other phosphatases should be kept to a minimum.

Compound 1 Augments ERK1/2 and p38 Activation in Human T Cells, Specifically by Inhibiting HePTP. For the

development of an HePTP chemical probe, essential criteria it must satisfy are that the compound be membrane-permeable and inhibit HePTP activity inside intact cells. In T cells, HePTP negatively regulates TCR signaling by dephosphorylating the activation loops of ERK1/2 and p38. Therefore, *bona fide* HePTP inhibitors should affect TCR-induced activation levels of ERK/p38. In order to probe ERK1/2 and p38 phosphorylation, we incubated Jurkat TAg T cells with selected compounds or vehicle (DMSO) at 37 °C for 45 min. Cells were then TCR-stimulated (with OKT3) for 5 min, and reactions were stopped by adding lysis buffer. Immunoblotting was carried out using phospho-ERK1/2 (*p*ERK1/2)- and phospho-p38 (*pp*38)-specific antibodies. In order to assess the specificity of the inhibitors, we also included a blot for phosphorylated mitogen activated protein kinase kinase (*p*MEK), which directly phosphorylates/activates ERK1/2. Therefore, by verifying unchanged MEK activation, augmented *p*ERK1/2 levels should not be the result of increased kinase activity upstream of ERK1/2 within the MAPK signaling cascade.

The immunoblotting results show that compound **1** augmented *p*ERK1/2 and *pp*38 levels, while activation of MEK was unchanged (Figure 5a). Additionally, we tested three analogues (compounds **3**, **4**, **5**), which also increased *p*ERK1/2 and *pp*38 levels (Figure 5a). Interestingly, compound **5**, which only modestly inhibited HePTP in the *in vitro* assay (IC$_{50}$ value of 35 μM), caused substantial augmentation of *p*ERK1/2. However, *p*MEK levels were also augmented in the presence of compound **5**, suggesting off-target effects of compound **5** upstream of ERK1/2. We then subjected compound **1** to a dose−response immunoblot experiment, using a similar assay format (Figure 5b). The effect of compound **1** on ERK1/2 and
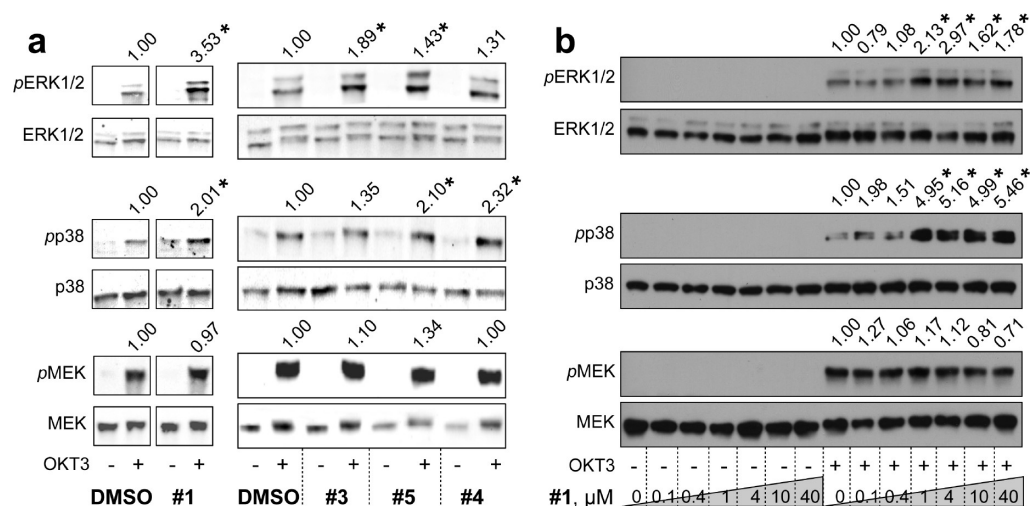
Figure 5. Screening of HePTP inhibitors in human T cells. (a) Probing ERK1/2 and p38 phosphorylation in Jurkat TAg T cells in the presence of vehicle (DMSO, 0.2%) or compound **1**, **3**, **4**, or **5** (40 μM), using phospho-specific antibodies against pT202/Y204-ERK1/2 (pERK1/2) and pT180/Y182-p38 (pp38). An anti-phospho-MEK (pMEK) blot was included as a specificity control. (b) Dose-response of compound **1**. Cell lysates were probed as in panel a. Phospho-protein bands were normalized to total protein levels. Statistical significance was determined by Student's t test (*$p < 0.05$). Representative blots are shown from 3 independent experiments.
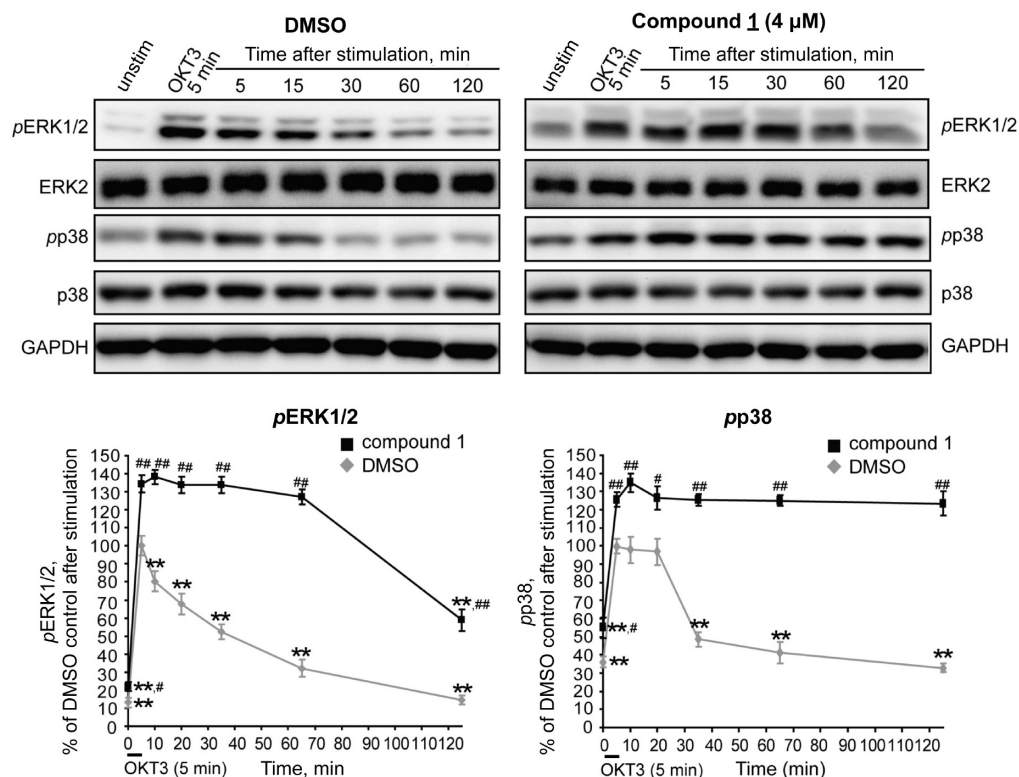

Figure 6. Compound **1** causes sustained hyperactivation of ERK1/2 and p38 in human T cells. ERK1/2 and p38 phosphorylation in Jurkat TAg T cells, preincubated with vehicle (DMSO, 0.2%) or compound **1** (4 μM), at various time points after TCR stimulation. Phospho-protein bands were normalized to total protein levels and then to GAPDH. Statistical significance was determined by one-way ANOVA with post hoc Tukey's test (within group (compound **1**- or DMSO-treated samples, respectively), **$p < 0.01$), or Student's t test (between groups (between compound **1**- and DMSO-treated samples), #$p < 0.05$, ##$p < 0.01$). Representative blots are shown from 4 independent experiments.

p38 activation was clearly dose-dependent and peaked between an inhibitor concentration of 1 and 4 μM. Given that pMEK levels were not affected, even at compound concentrations as high as 40 μM, off-target effects of compound **1** on molecules upstream of ERK1/2 can be excluded. MKP-3 is the only other known highly expressed PTP in T cells that acts on ERK1/2 early after TCR stimulation.[35] Compound **1** is 25-fold less

potent against recombinant MKP-3 (IC$_{50}$ = 5.2 μM) compared to HePTP. Thus, compound **1**, at concentrations between 1 and 4 μM, is not expected to significantly inhibit MKP-3 in cells. These results suggest that the observed effect of compound **1** on ERK1/2 activation in human T cells can be attributed to inhibition of HePTP.

Inhibition of HePTP Causes Sustained Hyperactivation of ERK1/2 and p38. A prolonged activation of MAPKs could be therapeutically valuable in cancer treatment. Therefore, we tested whether pharmacological inhibition of HePTP in T cells would sustain high levels of ERK1/2 and p38 activation after TCR stimulation. Preincubation of cells with compound **1** at 4 μM led to an increase in basal phosphorylation levels of both pERK1/2 and pp38 compared to the DMSO control (Figure 6; pERK1/2, 22.0 $\pm$ 2.5% vs 13.2 $\pm$ 2.7%, $p < 0.05$; pp38, 55.0 $\pm$ 5.8% vs 36.1 $\pm$ 3.1%, $p < 0.05$). TCR stimulation with OKT3 led to increases of pERK1/2 and pp38 levels in both DMSO- and compound-treated cells. However, phosphorylation levels were significantly higher in the presence of the inhibitor (pERK1/2: compound **1**, 134.3 $\pm$ 4.9%; DMSO, 100.0 $\pm$ 5.4%, $p < 0.01$; pp38: compound **1**, 125.5 $\pm$ 4.0%; DMSO, 100.0 $\pm$ 4.3%, $p < 0.01$). In the vehicle-treated cells, pERK1/2 levels rapidly decreased starting immediately after stimulation. On the other hand, pERK1/2 levels remained constant up to 1 h after stimulation in cells treated with compound **1** and only then started decreasing. Two hours after stimulation pERK1/2 levels were still significantly higher in the inhibitor-treated samples compared to the DMSO control. Similarly, pp38 levels started decreasing rapidly 15 min after stimulation in vehicle-treated cells, while pp38 levels remained unchanged in cells treated with compound **1**, even at 2 h after stimulation. Considering that nuclear MKPs that act on ERK/p38 at later time points (>30 min after TCR stimulation) are structurally similar to MKP-3, *i.e.*, they are missing the loop that corresponds to the SB-loop in HePTP, which is important for inhibitor binding, compound **1** will likely affect these MKPs at levels similar to MKP-3. Thus, at the used concentration of 4 μM, compound **1** is not expected to significantly inhibit other MKPs. Taken together, our results suggest that inhibition of HePTP in T cells not only augments but also sustains activation of ERK1/2 and p38.

Pharmacokinetic (PK) Analysis of Compound 1. The goal of these studies was to generate a chemical probe for HePTP that could also be utilized *in vivo*. Therefore, we assessed metabolic stability of compound **1** by monitoring its depletion over time while incubating it with rat liver microsomes in the presence of NADPH along with a reference compound of known microsomal half-life. LC−MS analysis was used and indicated a stability of 86.2 $\pm$ 2.7% after 15 min, 71.0 $\pm$ 2.9% after 30 min, and 53.0 $\pm$ 1.4% after 45 min. The half-life ($t_{1/2}$) of the inhibitor was calculated from its decrease with time to $t_{1/2}$ = 50 min, assuming first order kinetics (Figure 7a). Thus, compound **1** exhibited a metabolic stability that was sufficient for *in vivo* studies.[36−38] In addition, no major metabolite of compound **1** was identified in these studies. Rather, the compound metabolizes into multiple low-molecular-weight degradation products, as determined by LC−MS.

To determine the achievable concentration of compound **1** *in vivo*, we injected mice intraperitoneally (i.p.) with the inhibitor at 3 mg/kg and collected blood serum after 5, 20, 60, and 120 min. LC−MS analysis was used to determine serum concentrations, which showed the typical time course for a compound that is injected into the body cavity and must cross tissue in order to get into the systemic circulation (Figure 7b). Inhibitor concentration peaked at 20 min (1.24 $\pm$ 0.17 μM) and then decreased over the course of 2 h (0.018 $\pm$ 0.010 μM). Thus, given the peak activity of compound **1** in cells at concentrations between 1 and 4 μM, our results suggest that 3
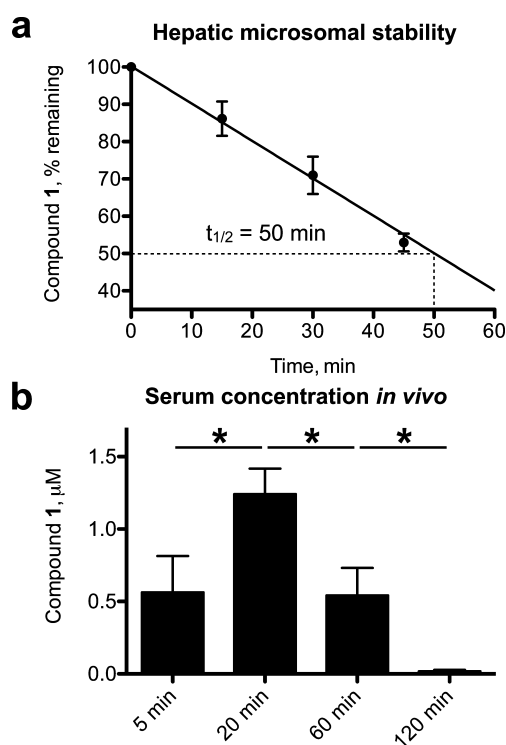
Figure 7. Pharmacokinetic (PK) analysis of compound **1**. (a) Hepatic microsomal stability of compound **1**. The half-life ($t_{1/2}$) of the inhibitor was calculated from its decrease with time, using linear regression. (b) Serum concentration of compound **1** in mice injected (i.p.) with compound **1** at 3 mg/kg; blood serum was collected after 5, 20, 60, and 120 min.

mg/kg or a slightly higher dosage is appropriate for *in vivo* studies.

Compound 1 Augments ERK1/2 and p38 Activation in Vivo. To test whether compound **1** was able to inhibit HePTP activity *in vivo*, we injected mice (i.p.) with compound **1** at 3 or 5 mg/kg and processed spleen at 3 or 6 h. Presence of the compound in the splenocytes was verified by LC−MS analysis. The inhibitor was detected in significant amounts 6 h after injection (0.265 $\pm$ 0.119 μM), indicating that clearance in the spleen tissue is lower than in the blood. Phosphorylation levels of ERK1/2 and p38 were assessed by immunoblot analysis using phospho-specific antibodies (Figure 8, upper panel). Leukocytes from inhibitor-treated mice exhibited significant higher activation levels of both ERK1/2 and p38 compared to vehicle controls (pERK1/2: 3 mg/kg for 6 h, 2.26 $\pm$ 0.46, $p < 0.05$; 5 mg/kg for 6 h, 1.97 $\pm$ 0.16, $p < 0.01$; pp38: 3 mg/kg for 3 h, 1.67 $\pm$ 0.16, $p < 0.01$; 3 mg/kg for h, 1.75 $\pm$ 0.13, $p < 0.01$; 5 mg/kg for 6 h, 2.33 $\pm$ 0.33, $p < 0.05$). Given a maximal serum concentration of compound **1** of 1.24 μM (at 3 mg/kg dosage) and an even lower concentration in the spleen tissue (<0.5 μM), it is unlikely that the ERK1/2 and p38 hyperactivation is due to inhibition of PTPs other than HePTP.

To further address specificity of compound **1**, we also determined phosphorylation of AKT, a key signaling molecule downstream of CD28/PI3K in a pathway that leads to NF-kB activation. There was no change in AKT phosphorylation levels at the doses and time points used (Figure 8, lower panel). Since HePTP activity is regulated by phosphorylation at Ser23 by PKA,[17] we also probed this site with a phospho-specific antibody.[20] No changes in phospho-HePTP levels were detected, indicating that the augmented MAPK activation was
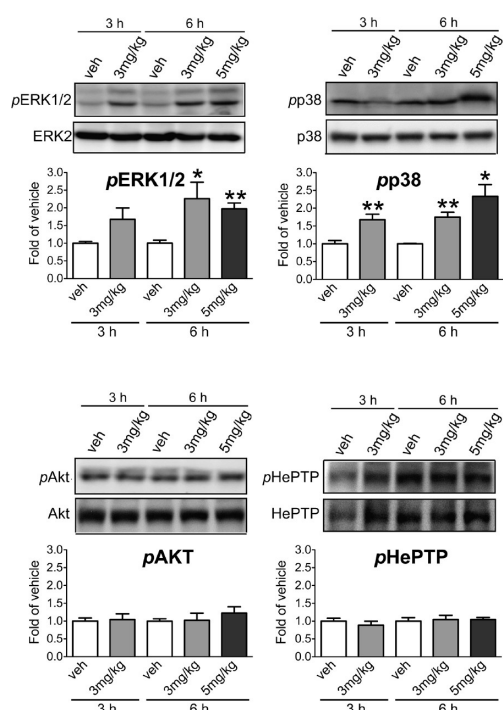
Figure 8. Compound **1** augments ERK1/2 and p38 activation *in vivo*. ERK1/2 and p38 phosphorylation in spleenocytes of mice injected (i.p.) with compound **1** or vehicle. Total lysates from spleen were probed with phospho-specific antibodies against $pT202/Y204$-ERK1/2 ($pERK1/2$), $pT180/Y182$-p38 ($pp38$), $pS473$-AKT1 ($pAKT$), and $pS23$-HePTP ($pHePTP$). Phosphorylation levels were normalized to total protein, then to GAPDH as a loading control. ($*p < 0.05$, $**p < 0.01$, $n = 4$).

not due to disruption of the HePTP/MAPK complex as a result of the phosphorylation of the regulatory serine within the KIM (Figure 8, lower panel).

Finally, since the PTPs most similar to HePTP, PTP-SL and STEP, are exclusively expressed in the brain,[39] we tested whether compound **1** could cross the blood-brain-barrier (BBB) and potentially inhibit these phosphatases. Brain tissue from mice injected with compound **1** (i.p.) at 3 or 5 mg/kg was processed 3 h after injection. Using LC−MS analysis, compound **1** could not be detected in the brain tissue (the detection limit was ∼1 nM). Also when we specifically analyzed the cerebellum, the part of the brain where PTP-SL is expressed, compound **1** could not be detected. Thus, compound **1** does not appear to cross the BBB. Taken together, we showed that compound **1** may be used as a chemical probe for HePTP *in vivo*. Future studies of compound **1** in mouse models of acute leukemia are warranted.

Compound 1 Complies with Essential Criteria of a Chemical Probe. A common understanding of what makes a compound a chemical probe was lacking until recently, when Stephen Frye proposed a set of principles to guide probe qualification.[29] His five requirements for a high quality chemical probe include (1) molecular profiling, (2) mechanism of action, (3) identity of the active species, (4) proven utility as a probe, and (5) availability. Compound **1** meets all of these criteria. First, we provide comprehensive molecular profiling data. Specifically, we show that compound **1** is highly potent *in vitro*, in human T cells, and *in vivo*, and significant effects in cells and *in vivo* can be achieved with a relatively low dose of the inhibitor, compared to its *in vitro* IC_{50} value. Moreover, the

compound demonstrates between 5- and 30-fold selectivity for HePTP over the most similar enzymes in the *in vitro* assay and shows no signs of an off-target effect in the cell-based or *in vivo* experiments. Second, we determined the mechanism of action of compound **1** on the atomic level, *i.e.*, the binding mode between the inhibitor and the protein. In addition, the effect of the inhibitor is dose-dependent in all experiments in which it was tested. Third, compound **1** is the active species that inhibits HePTP as no degradation of compound **1** was observed in the *in vitro* assays, and LC−MS analysis revealed no major metabolites of the compound in the stability assay (only multiple low-molecular-weight degradation products were found). These data suggest that observed effects *in vivo* are due to compound **1** as the active species. Fourth, the utility of compound **1** as a chemical probe was demonstrated. Namely, the compound was utilized to show, for the first time, that pharmacological inhibition of HePTP not only augments but also sustains ERK1/2 and p38 activation in human T cells and in leukocytes *in vivo*. And fifth, the compound is readily available to the academic community.

In conclusion, we have developed a potent and relatively specific chemical probe for HePTP, a critical negative regulator of the MAPKs ERK1/2 and p38 in hematopoietic cells. To our knowledge, this is the first time that a small-molecule inhibitor of a protein tyrosine phosphatase has been successfully utilized to control MAPK activation *in vivo*. Current investigations are underway to determine whether compound **1** can be developed into a treatment strategy for hematopoietic malignancies such as AML or T-ALL.

■ METHODS

Materials. p-Nitrophenyl phosphate (pNPP), 3-O-methylfluorescein phosphate (OMFP), dithiothreitol (DTT), and sodium orthovanadate (Na_3VO_4) were purchased from Sigma-Aldrich. Biomol Green reagent was from Biomol Research Laboratories, Inc. Compound **1** was repurchased from Labotest (no. LT00237558), and analogues were ordered from ChemBridge. All compounds had a purity of >95% (verified by LC−MS and ^{1}H NMR). All other chemicals and reagents were of the highest grade available commercially. All antibodies in the T cell *in vitro* assays were from Cell Signaling Technology Inc. Antibodies used in the experiments with mouse tissue are listed in Supplementary Table S1. For recombinant proteins see Supplementary Methods.

Chemical Library Screening and Dose−Response Assays. See Supplementary Methods.

Dose−Response Inhibitor Studies Using OMFP. Phosphatase activity was measured in a 384- or 96-well format assay system. Compounds were 2-fold serially diluted in DMSO before being added to the reactions for a 10-point dose−response curve. Reactions contained 50 mM Bis-Tris pH 6.0, 1.7 mM DTT, 0.005% Tween 20, and 5% DMSO. OMFP concentrations (corresponding to the K_m value of each enzyme) were 117 μM for HePTP (2.75 nM), 50 μM for MKP-3 (1 μg mL^{-1}), 12.5 μM for VHR (3 nM), 35 μM for STEP (5 nM), 28 μM for PTP-SL (5 nM), 99 μM for PTP1B (10 nM), 184 μM for LYP (5 nM), 144 μM for HePTP-DM (5 nM), and 222 μM for HePTP H237A (5 nM). Fluorescence intensity was measured in kinetic mode over 10 min to determine the slopes of progress curves, using an Envision plate reader (PerkinElmer), an excitation wavelength of 485 nm, and an emission wavelength of 528 nm. IC_{50} values were determined using nonlinear regression (sigmoidal dose-response with variable slope) and the program Prism (v5.0b GraphPad Software, Inc.).

Michaelis−Menten Kinetic Studies tTo Determine the Inhibition Mode of Compound 1. The HePTP-catalyzed hydrolysis of OMFP was assayed at RT in a 60 μL 96-well format reaction system in 50 mM Bis-Tris, pH 6.0 assay buffer containing 1.7 mM

DTT, 0.005% Tween-20, and 5% DMSO. Recombinant HePTP (5 nM) was preincubated with various fixed concentrations of inhibitor (0, 0.1, 0.2, 0.4, 0.8, 1.6, 3.2 μM) for 10 min. The reaction was initiated by addition of various concentrations of substrate (0, 12.5, 25, 50, 100, 200, 400 μM) to the reaction mixture. The initial rate was determined using an FLx800 micro plate reader (Bio-Tek Instruments, Inc.) using an excitation wavelength of 485 nm and measuring the emission of the fluorescent reaction product at 528 nm. The nonenzymatic hydrolysis of the substrate was corrected by measuring the control without addition of enzyme. Eadie-Hofstee plots were generated using the program Prism (v5.0b GraphPad Software, Inc.). The inhibition pattern and inhibition constant were determined as described previously.[40] For a comparison of the fitting results the second-order Akaike's Information Criterion (AICc) was calculated with eq 1, where N is the number of data points, SS is the absolute sum of squares, and K is the number of parameters fit by nonlinear regression plus 1.

$$AICc = N \ln(SS/N) + 2K + (2K(K+1))$$
$$/(N - K - 1) \tag{1}$$

The probability to have chosen the right model can be computed by eq 2, where & is the difference between AICc scores.

$$\text{probability} = \exp(-0.5\&)/(1 + \exp(-0.5\&)) \tag{2}$$

Generation of HePTP K105A/T106A Double Mutant and HePTP H237A Mutant. See Supplementary Methods.

In Silico **Docking Studies.** Flexible ligand docking calculations were performed on a MacPro workstation with the ICM docking algorithm[41] as implemented in the ICM-Pro program (v3.7-1g, Molsoft, LLC.). The coordinates of the three-dimensional (3D) structure of HePTP (PDB code 3D44, ref 34), MKP-3 (PDB code 1MKP), and STEP (PDB code 2BV5) were converted into ICM objects, charges were assigned, orientations of side chain amides were corrected, and hydrogen atoms were added and their positions optimized by energy minimization using MMFF force field. Mutations in the crystal structures were corrected to wt amino acid sequences, and the side chains were optimized using the Optimize Side Chains tool as implemented in ICM-Pro. The binding pockets were defined as follows. HePTP: residues in an 8 Å radius around the pTyr of the peptide ligand; MKP-3 and STEP: residues in an 10 Å radius around the catalytic Cys. Energy-minimized 3D molecular models of the compounds were generated with the implemented routine in ICM.

TCR Stimulation, Cell Lysis, and Immunoblotting. Jurkat TAg T cells were treated either with small molecule compound or with DMSO alone (vehicle control) for 45 min at 37 °C. Cells were then TCR-stimulated with an optimal dose of OKT3 (500 ng mL^{-1}) for 5 min. Thereafter, cells were either washed with RPMI 1640 medium and incubated in fresh medium for the indicated period of time (experiment in Figure 6) or immediately lysed in lysis buffer (50 mM HEPES, pH 7.4, 100 mM NaCl, 1% Triton X-100, 50 mM NaF, 5 mM Na$_3$VO$_4$, 1 mM PMSF, 5 mM EDTA), before proteins were separated using SDS-PAGE, transferred onto PVDF membranes, and blotted with the indicated antibodies. These procedures were carried out as described previously.[42] Densitometric quantifications were performed using either ImageJ (http://rsbweb.nih.gov/ij, Figure 5) or the Genetools program (Syngene, Figure 6). Data are expressed as means ± SEM. Statistical significance (*$p < 0.05$, ** $p < 0.01$) was determined by Student's t test.

PK Analysis. See Supplementary Methods.

In Vivo **Testing of Compound 1.** The Yale University Institutional Animal Care and Use Committee approved all animal procedures. C57B6 mice (3 mice at each dose and time, Jackson Laboratory) were injected with compound **1** (i.p., 3 or 5 mg kg^{-1}) or vehicle and were sacrificed 3 or 6 h postinjection. Spleen, cerebellum, and cortex were processed for biochemical assays. Spleen was lysed in sonication buffer (50 mM Tris pH 7.4, 150 mM NaCl, 5 mM NaF, 1 mM Na$_3$VO$_4$, 1 mM EDTA, 1 mM EGTA and protease inhibitor cocktail (Roche)) with brief sonication. Lysates were spun at 800g for 10 min, and supernatants were kept for Western blotting. Cerebellum and cortex were homogenized in TEVP buffer (10 mM Tris pH 7.4, 5

mM NaF, 1 mM Na$_3$VO$_4$, 1 mM EDTA, 1 mM EGTA and protease inhibitor cocktail). Homogenates were centrifuged at 1000g for 10 min, and supernatants (S1) were further centrifuged at 10,000g for 15 min to obtain a crude synaptosomal fraction (P2). P2 pellets were subsequently resuspended and lysed in TEVP buffer. Protein concentrations were determined with the BCA kit (Thermo Fisher Scientific). For Western blotting, samples were prepared in sample buffer (Biorad), resolved by SDS-PAGE, transferred to nitrocellulose membrane, and incubated with primary antibodies listed in Supplementary Table S1 overnight at 4 °C. Membranes were washed and incubated in peroxidase-conjugated secondary antibodies. The immunoreactivities were visualized using a Chemiluminescent substrate kit (Thermo Fisher Scientific) and detected using G:BOX with the image program GeneSnap (Syngene). All densitometric quantifications were obtained using the Genetools program (Syngene). Data are expressed as means ± SEM. Statistical significance ($p < 0.05$) was determined by one-way ANOVA with post hoc Tukey's test or Student's t test. All experiments were repeated at least three times.

■ ASSOCIATED CONTENT

⑤ Supporting Information

This material is available free of charge *via* the Internet at http://pubs.acs.org.

■ AUTHOR INFORMATION

Corresponding Author
*E-mail: tautz@burnham.org.

Author Contributions
#These authors contributed equally to this work.

■ ACKNOWLEDGMENTS

■ ABBREVIATIONS

DTT, dithiothreitol; ERK, extracellular signal-regulated kinase; HePTP, hematopoietic protein tyrosine phosphatase; MAPK, mitogen-activated protein kinase; MKP, MAPK phosphatase; OMFP, 3-O-methylfluorescein phosphate; pTyr, phosphotyrosine; pNPP, p-nitrophenyl phosphate; PTK, protein tyrosine kinase; PTP, protein tyrosine phosphatase; SAR, structure—activity relationship; TCR, T cell antigen receptor

■ REFERENCES

(1) Hunter, T., and Sefton, B. M. (1980) Transforming gene product of Rous sarcoma virus phosphorylates tyrosine. *Proc. Natl. Acad. Sci. U.S.A. 77*, 1311−1315.

(2) Alonso, A., Sasin, J., Bottini, N., Friedberg, I., Friedberg, I., Osterman, A., Godzik, A., Hunter, T., Dixon, J., and Mustelin, T. (2004) Protein tyrosine phosphatases in the human genome. *Cell 117*, 699−711.

(3) Mustelin, T., Vang, T., and Bottini, N. (2005) Protein tyrosine phosphatases and the immune response. *Nat. Rev. Immunol. 5*, 43−57.

(4) Tonks, N. K. (2006) Protein tyrosine phosphatases: from genes, to function, to disease. *Nat. Rev. Mol. Cell. Biol. 7*, 833−846.

(5) Tautz, L., Pellecchia, M., and Mustelin, T. (2006) Targeting the PTPome in human disease. *Expert Opin. Ther. Targets 10*, 157−177.

375

dx.doi.org/10.1021/cb2004274 | *ACS Chem. Biol.* 2012, 7, 367−377

(6) Saxena, M., and Mustelin, T. (2000) Extracellular signals and scores of phosphatases: all roads lead to MAP kinase. *Semin. Immunol.* 12, 387−396.

(7) Canagarajah, B. J., Khokhlatchev, A., Cobb, M. H., and Goldsmith, E. J. (1997) Activation mechanism of the MAP kinase ERK2 by dual phosphorylation. *Cell* 90, 859−869.

(8) Kyriakis, J. M., and Avruch, J. (2001) Mammalian mitogen-activated protein kinase signal transduction pathways activated by stress and inflammation. *Physiol. Rev. 81,* 807−869.

(9) Denu, J. M., Zhou, G., Wu, L., Zhao, R., Yuvaniyama, J., Saper, M. A., and Dixon, J. E. (1995) The purification and characterization of a human dual-specific protein tyrosine phosphatase. *J. Biol. Chem. 270,* 3796−3803.

(10) Alonso, A., Merlo, J. J., Na, S., Kholod, N., Jaroszewski, L., Kharitonenkov, A., Williams, S., Godzik, A., Posada, J. D., and Mustelin, T. (2002) Inhibition of T cell antigen receptor signaling by VHR-related MKPX (VHX), a new dual specificity phosphatase related to VH1 related (VHR). *J. Biol. Chem. 277,* 5524−5528.

(11) Alessi, D. R., Gomez, N., Moorhead, G., Lewis, T., Keyse, S. M., and Cohen, P. (1995) Inactivation of p42 MAP kinase by protein phosphatase 2A and a protein tyrosine phosphatase, but not CL100, in various cell lines. *Curr. Biol. 5,* 283−295.

(12) Zhou, B., Wang, Z. X., Zhao, Y., Brautigan, D. L., and Zhang, Z. Y. (2002) The specificity of extracellular signal-regulated kinase 2 dephosphorylation by protein phosphatases. *J. Biol. Chem. 277,* 31818−31825.

(13) Cerignoli, F., Rahmouni, S., Ronai, Z., and Mustelin, T. (2006) Regulation of MAP kinases by the VHR dual-specific phosphatase: implications for cell growth and differentiation. *Cell Cycle 5,* 2210−2215.

(14) Zanke, B., Suzuki, H., Kishihara, K., Mizzen, L., Minden, M., Pawson, A., and Mak, T. W. (1992) Cloning and expression of an inducible lymphoid-specific, protein tyrosine phosphatase (HePTPase). *Eur. J. Immunol. 22,* 235−239.

(15) Adachi, M., Sekiya, M., Isobe, M., Kumura, Y., Ogita, Z., Hinoda, Y., Imai, K., and Yachi, A. (1992) Molecular cloning and chromosomal mapping of a human protein-tyrosine phosphatase LC-PTP. *Biochem. Biophys. Res. Commun. 186,* 1607−1615.

(16) Saxena, M., Williams, S., Brockdorff, J., Gilman, J., and Mustelin, T. (1999) Inhibition of T cell signaling by mitogen-activated protein kinase-targeted hematopoietic tyrosine phosphatase (HePTP). *J. Biol. Chem. 274,* 11693−11700.

(17) Saxena, M., Williams, S., Tasken, K., and Mustelin, T. (1999) Crosstalk between cAMP- dependent kinase and MAP kinase through a protein tyrosine phosphatase. *Nat. Cell Biol. 1,* 305−311.

(18) Gronda, M., Arab, S., Iafrate, B., Suzuki, H., and Zanke, B. W. (2001) Hematopoietic protein tyrosine phosphatase suppresses extracellular stimulus-regulated kinase activation. *Mol. Cell. Biol. 21,* 6851−6858.

(19) Pettiford, S. M., and Herbst, R. (2003) The protein tyrosine phosphatase HePTP regulates nuclear translocation of ERK2 and can modulate megakaryocytic differentiation of K562 cells. *Leukemia 17,* 366−378.

(20) Nika, K., Hyunh, H., Williams, S., Paul, S., Bottini, N., Tasken, K., Lombroso, P. J., and Mustelin, T. (2004) Haematopoietic protein tyrosine phosphatase (HePTP) phosphorylation by cAMP-dependent protein kinase in T-cells: dynamics and subcellular location. *Biochem. J. 378,* 335−342.

(21) Gjorloff-Wingren, A., Saxena, M., Han, S., Wang, X., Alonso, A., Renedo, M., Oh, P., Williams, S., Schnitzer, J., and Mustelin, T. (2000) Subcellular localization of intracellular protein tyrosine phosphatases in T cells. *Eur. J. Immunol. 30,* 2412−2421.

(22) Zanke, B., Squire, J., Griesser, H., Henry, M., Suzuki, H., Patterson, B., Minden, M., and Mak, T. W. (1994) A hematopoietic protein tyrosine phosphatase (HePTP) gene that is amplified and overexpressed in myeloid malignancies maps to chromosome 1q32.1. *Leukemia 8,* 236−244.

(23) Fonatsch, C., Haase, D., Freund, M., Bartels, H., and Tesch, H. (1991) Partial trisomy 1q. A nonrandom primary chromosomal abnormality in myelodysplastic syndromes? *Cancer Genet. Cytogenet. 56,* 243−253.

(24) Mamaev, N., Mamaeva, S. E., Pavlova, V. A., and Patterson, D. (1988) Combined trisomy 1q and monosomy 17p due to translocation t(1;17) in a patient with myelodysplastic syndrome. *Cancer Genet. Cytogenet. 35,* 21−25.

(25) Bobkova, E. V., Liu, W. H., Colayco, S., Rascon, J., Vasile, S., Gasior, C., Critton, D. A., Chan, X., Dahl, R., Su, Y., Sergienko, E., Chung, T. D. Y., Mustelin, T., Page, R., and Tautz, L. (2011) Inhibition of the hematopoietic protein tyrosine phosphatase by phenoxyacetic acids. *ACS Med. Chem. Lett. 2,* 113−118.

(26) Eswaran, J., von Kries, J. P., Marsden, B., Longman, E., Debreczeni, J. E., Ugochukwu, E., Turnbull, A., Lee, W. H., Knapp, S., and Barr, A. J. (2006) Crystal structures and inhibitor identification for PTPN5, PTPRR and PTPN7: a family of human MAPK-specific protein tyrosine phosphatases. *Biochem. J. 395,* 483−491.

(27) Wagner, E. F., and Nebreda, A. R. (2009) Signal integration by JNK and p38 MAPK pathways in cancer development. *Nat. Rev. Cancer 9,* 537−549.

(28) Barglow, K. T., and Cravatt, B. F. (2007) Activity-based protein profiling for the functional annotation of enzymes. *Nat. Methods 4,* 822−827.

(29) Frye, S. V. (2010) The art of the chemical probe. *Nat. Chem. Biol. 6,* 159−161.

(30) Tautz, L., and Mustelin, T. (2007) Strategies for developing protein tyrosine phosphatase inhibitors. *Methods 42,* 250−260.

(31) Barr, A. J., Ugochukwu, E., Lee, W. H., King, O. N., Filippakopoulos, P., Alfano, I., Savitsky, P., Burgess-Brown, N. A., Muller, S., and Knapp, S. (2009) Large-scale structural analysis of the classical human protein tyrosine phosphatome. *Cell 136,* 352−363.

(32) Vintonyak, V. V., Antonchick, A. P., Rauh, D., and Waldmann, H. (2009) The therapeutic potential of phosphatase inhibitors. *Curr. Opin. Chem. Biol. 13,* 272−283.

(33) Willett, P. (2006) Similarity-based virtual screening using 2D fingerprints. *Drug Discovery Today 11,* 1046−1053.

(34) Critton, D. A., Tortajada, A., Stetson, G., Peti, W., and Page, R. (2008) Structural basis of substrate recognition by hematopoietic tyrosine phosphatase. *Biochemistry 47,* 13336−13345.

(35) Arimura, Y., and Yagi, J. (2010) Comprehensive expression profiles of genes for protein tyrosine phosphatases in immune cells. *Sci. Signaling 3,* rs1.

(36) Obach, R. S. (1999) Prediction of human clearance of twenty-nine drugs from hepatic microsomal intrinsic clearance data: An examination of in vitro half-life approach and nonspecific binding to microsomes. *Drug Metab. Dispos. 27,* 1350−1359.

(37) McGinnity, D. F., Soars, M. G., Urbanowicz, R. A., and Riley, R. J. (2004) Evaluation of fresh and cryopreserved hepatocytes as in vitro drug metabolism tools for the prediction of metabolic clearance. *Drug Metab. Dispos. 32,* 1247−1253.

(38) Yang, Z., Zadjura, L. M., Marino, A. M., D'Arienzo, C. J., Malinowski, J., Gesenberg, C., Lin, P. F., Colonno, R. J., Wang, T., Kadow, J. F., Meanwell, N. A., and Hansel, S. B. (2010) Utilization of in vitro Caco-2 permeability and liver microsomal half-life screens in discovering BMS-488043, a novel HIV-1 attachment inhibitor with improved pharmacokinetic properties. *J. Pharm. Sci. 99,* 2135−2152.

(39) Andersen, J. N., Mortensen, O. H., Peters, G. H., Drake, P. G., Iversen, L. F., Olsen, O. H., Jansen, P. G., Andersen, H. S., Tonks, N. K., and Moller, N. P. (2001) Structural and evolutionary relationships among protein tyrosine phosphatase domains. *Mol. Cell. Biol. 21,* 7117−7136.

(40) Tautz, L., Bruckner, S., Sareth, S., Alonso, A., Bogetz, J., Bottini, N., Pellecchia, M., and Mustelin, T. (2005) Inhibition of Yersinia tyrosine phosphatase by furanyl salicylate compounds. *J. Biol. Chem. 280,* 9400−9408.

(41) Abagyan, R., and Totrov, M. (1994) Biased probability Monte Carlo conformational searches and electrostatic calculations for peptides and proteins. *J. Mol. Biol. 235,* 983−1002.

(42) Alonso, A., Bottini, N., Bruckner, S., Rahmouni, S., Williams, S., Schoenberger, S. P., and Mustelin, T. (2004) Lck dephosphorylation at

Tyr-394 and inhibition of T cell antigen receptor signaling by Yersinia phosphatase YopH. *J. Biol. Chem. 279*, 4922−4928.